Structural Engineering and Mechanics, Vol. 31, No. 6 (2009) 697-716
DOI: http://dx.doi.org/10.12989/sem.2009.31.6.697

Seismic performance of high strength reinforced concrete columns

Hakim Bechtoula†

National Earthquake Engineering Center, C.G.S
01 Rue Kaddour Rahim, BP252 Hussein Dey, Alger, Algeria

Susumu Kono‡ and Fumio Watanabe‡†

Department of Architecture and Architectural Engineering, Kyoto University,
Nishikyo, Kyoto 6158540, Japan

(Received June 29, 2008, Accepted March 13, 2009)

Abstract. This paper summarizes an experimental and analytical study on the seismic behavior of high strength reinforced concrete columns under cyclic loading. In total six cantilever columns with different sizes and concrete compressive strengths were tested. Three columns, small size, had a 325 × 325 mm cross section and the three other columns, medium size, were 520 × 520 mm. Concrete compressive strength was 80, 130 and 180 MPa. All specimens were designed in accordance with the Japanese design guidelines. The tests demonstrated that, for specimens made of 180 MPa concrete compressive strength, spalling of cover concrete was very brittle followed by a significant decrease in strength. Curvature was much important for the small size than for the medium size columns. Concrete compressive strength had no effect on the curvature distribution for a drift varying between −2% and +2%. However, it had an effect on the drift corresponding to the peak moment and on the equivalent viscous damping variation. Simple equations are proposed for 1) evaluating the concrete Young's modulus for high strength concrete and for 2) evaluating the moment-drift envelope curves for the medium size columns knowing that of the small size columns. Experimental moment-drift and axial strain-drift histories were well predicted using a fiber model developed by the authors.

Keywords: column; high strength concrete; performance; scale effect; damping factor; curvature; capacity; damage.

1. Introduction

With the increased knowledge that has been gained with respect to material availability, design methodology, and construction techniques, the feasible realm of high-strength concrete applications has grown dramatically. In the 1950s, concrete with a compressive strength of 34 MPa was considered high strength. Today, high strength concrete is defined as concrete with a specified compressive strength of 55 MPa or higher (ACI Committee-363 2005). In many markets today,

† Ph.D., Corresponding author, E-mail: hbechtoula@cgs-dz.org, bechhakim@gmail.com
‡ Associate Professor, E-mail: kono@archi.kyoto-u.ac.jp
‡† Professor Emeritus, E-mail: nabe@archi.kyoto-u.ac.jp

concrete having a specified compressive strength in excess of 69 MPa is routinely produced on a daily basis. Although 55 MPa was selected as the current lower limit, it is not intended to imply that any drastic change in material properties or in production techniques occurs at this compressive strength. In reality, all changes that take place at or above 55 MPa represent a process which starts with the lower strength concretes and continues into the high strength realm.

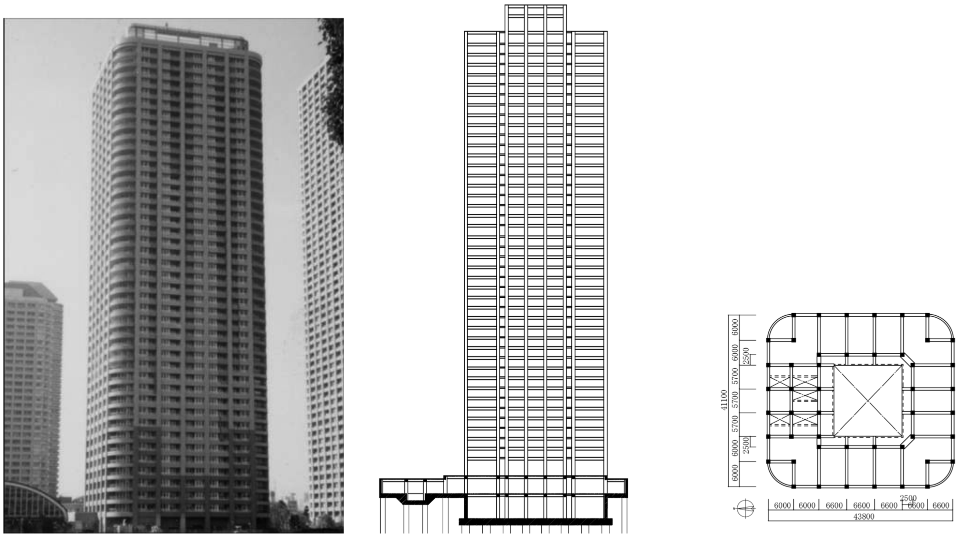

(a) View of the building (b) Vertical section (c) Horizontal section

Fig. 1 The River-City 21 North-Block N-building (f'_c = 100 MPa)

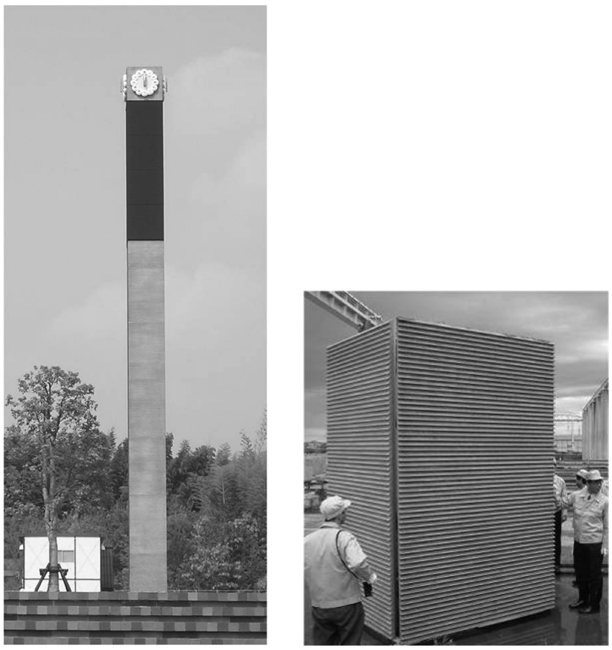

(a) Clock Tower (b) Precast unit

Fig. 2 The new Clock Tower at Katsura campus, Kyoto University (f'_c= 200 MPa)

In Japan, use of Reinforced Concrete (RC) structures to high-rise buildings has rapidly increased after the publication of the report of “New RC Project” (JICE 1988-1993). This project also took into account the results of many research program carried in the past (Nishiyama 1993, Kuramoto 1995, Muguruma 1990). The results of “New RC Project” and the succeeding progress of structural analyses and construction technology have made the realization of high-rise buildings of RC structures more possible. In 1997, concrete of specified compressive strength of 100 MPa was applied to the columns of the residential River-City 21 North-Block N-building (Namiki 1999) with 43 stories and 145 m in height as illustrated in Fig. 1. Recently, a new clock tower, shown in Fig. 2, with 30 m in height and a concrete compressive strength of 200 MPa was constructed at Katsura Campus, Kyoto University.

At the same campus, at Kyoto University, six high strength reinforced concrete columns with different sizes and concrete compressive strengths were tested under vertical and lateral loadings. This paper reports some of the main results drawn from this experiment.

2. Material characteristics and test setup

In total six high strength reinforced concrete cantilever columns, were designed according to the

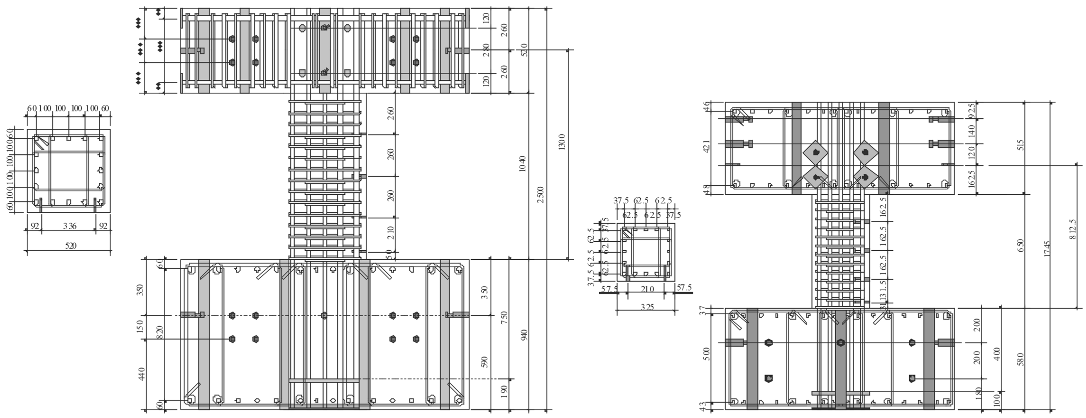

(a) Medium size (b) Small size

Fig. 3 Dimensions and steel arrangement of the specimens

Table 1 Specimens characteristics and test variables

Specimen	Column width D (mm)	Shear span (mm)	Shear span ratio	Concrete strength f'c (MPa)	Longitudinal rebar (ratio)	Shear rebar (ratio)	Normalized axial load ($N/f'cD^2$)
M180	520	1300	2.5	180	16D26 3.00 %	UD10@50 0.78 %	0.3
M130	520	1300		130			
M080	520	1300		80			
S180	325	812.5		180	16D16 3.00 %	UD6@50 0.78 %	
S130	325	812.5		130			
S080	325	812.5		80			

Table 2 Material characteristics

(a) Steel reinforcements

Identification	σ_y (Mpa)	σ_b (Mpa)	Es ($\times 10^5$) (Mpa)
SD 685 (D16)	757	967	1.95
SD 686 (D25)	729	925	1.96
UD6	964	1005	2.07
UD10	920	986	2.01

(b) Reinforced concrete

Specimen	Concrete strength (Mpa)	Ec (GPa)
M180	168	45.7
M130	131	43.1
M080	65.5	36.2
S180	170	46.5
S130	132	43
S080	68.2	34.8

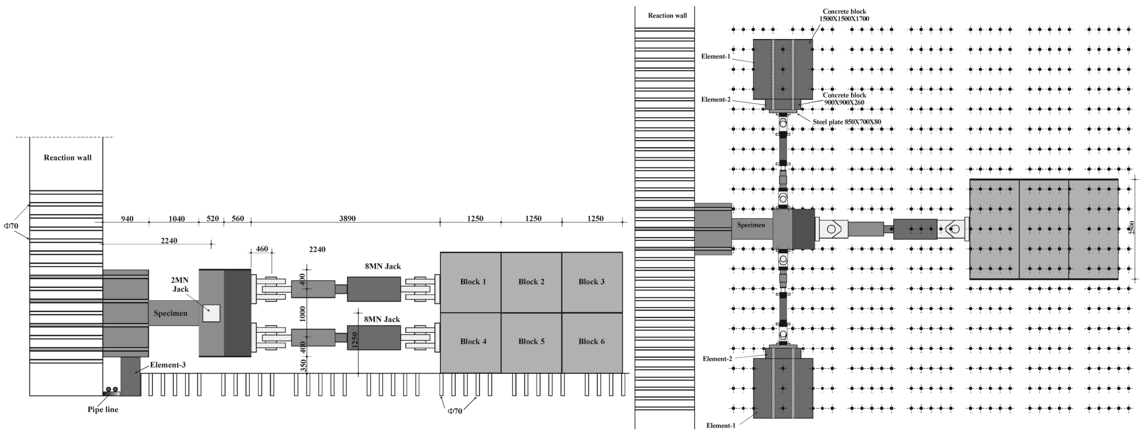

(a) Side view (b) Top view

Medium columns

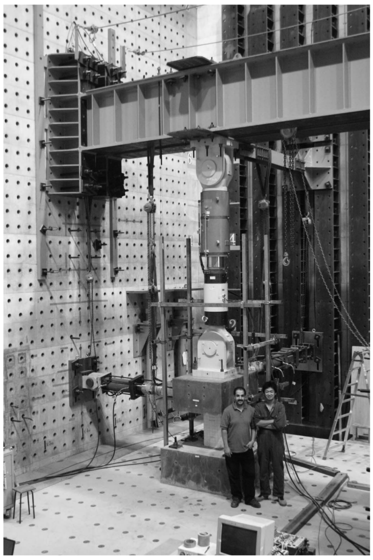

Small columns

Fig. 4 Test setup

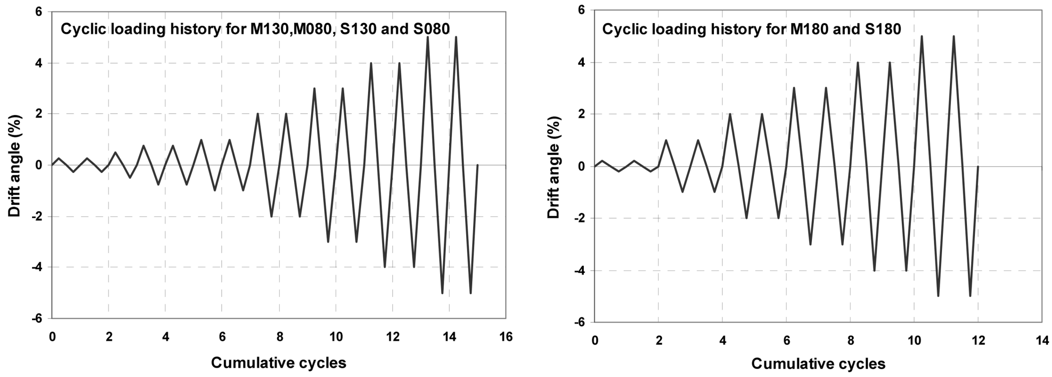

(a) 80 and 130 MPa columns (b) 180 MPa columns

Fig. 5 Loading history

Japanese guide lines (AIJ 1999) and tested at Kyoto University. Three specimens had a cross section of 325 × 325 mm, named small size columns, and the three others had a cross section of 520 × 520 mm, named medium size columns. Fig. 3 shows the geometry and the dimensions of the two types of columns. The test variables were the column dimensions and the concrete compressive strength. Shear span ratio, longitudinal and transversal reinforcement and the normalized axial load were the same for the medium and small columns. Three types of concrete strength were used in the experiment, 80, 130 and 180 MPa. Table 1 summarizes the specimen characteristics and the test variables. Concrete and steel mechanical characteristics are shown in Tables 2(a) and (b), respectively.

Due to the high axial load applied to the medium size columns, and in order to use the reaction wall and the reaction blocks, these specimens were tested in horizontal position as shown at the upper part of Fig. 4. Two 8 MN hydraulic jacks were used to apply the axial load and two 2 MN jacks to apply the reversed cyclic loading. Small size columns were tested vertically using the steel testing frame to apply the axial load, see Fig. 4.

Fig. 5 shows the reversed cyclic loading history applied during the test for the 6 specimens.

3. Experimental results

3.1 Variation of concrete Young's modulus

The modulus of elasticity, Young's modulus, can significantly influences the behavior of high strength concrete structure, and therefore, is a highly important mechanical property. In calculations for seismic design of reinforced concrete structures, calculated drift ratios are directly affected by the Young's modulus of the concrete used in the columns. The Young's modulus can be influenced by several mixture properties, including the compressive strength of the concrete, coarse aggregate content, and the mechanical properties of the coarse aggregate. In this section, effect of the concrete compressive strength on the Young' modulus is investigated.

Martinez *et al.* (Martinez 1982) proposed the following equation for evaluating the concrete Young's modulus for high strength concrete

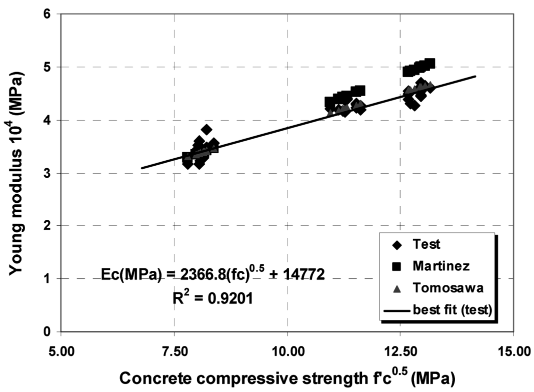

Fig. 6 Variation of Young's modulus

$$E_c = 3320\sqrt{f'_c} + 6900[\text{MPa}] \quad (1)$$

Tomosawa *et al.* (Tomosawa 1995) proposed also an equation for evaluating the Young modulus for high strength concrete in the following form

$$E_c = 33500 \cdot K_1 \cdot K_2 \cdot \left(\frac{\rho}{2.4}\right)^2 \left(\frac{f'_c}{60}\right)^{1/3} \quad (2)$$

where, E_c and f'_c are respectively the concrete Young's modulus, K_1, K_2 and ρ are the parameter depending on the concrete mixture and the concrete density, respectively.

Fig. 6 shows the concrete Young's modulus variation obtained from 54 tested cylinders taken from the same batch used to make the specimens. These values are compared on the same figure to Eq. (1) and Eq. (2). As it can be seen Martinez *et al.* equation gives a good estimation of the Young's modulus for a concrete having a compressive strength of 80 MPa, however, beyond that the results are overestimated. Tomosawa equation gives a very good estimation for the Young's modulus as illustrated in the figure for all tested cylinders.

Based on the 54 tested cylinders, a similar equation to that proposed by Martinez *et al.* for evaluating the concrete Young's modulus is proposed for concrete having a compressive strength higher than 80 MPa. The proposed equation is formulated as

$$E_c = 2366.8\sqrt{f'_c} + 14772[\text{MPa}] \quad (3)$$

Eq. (3) had a coefficient of covariance (the R-squared value) higher than 92%.

3.2 Load-drift and axial strain variation

Experimental horizontal load-drift and axial strain-drift are illustrated in Fig. 7 and Fig. 8 for the medium and small size columns, respectively. Axial strains were measured using the displacement gauges set at the lower part of the columns shown in Fig. 11. Spalling of the concrete cover was very brittle especially for specimens with 130 and 180 MPA. These stages are indicated with dots marks on the load-drift relationship curves. After the spalling, the horizontal bearing capacity of specimens with 130 and 180 MPa concrete strength decreased significantly. However, for specimens

M080 and S080 the horizontal load increased after spalling of the cover concrete.

The right side of Fig. 7 and Fig. 8 show the axial strain (shortening and/or elongation) variation computed at the center of the column's sections. Shortening of the column has a positive sign in the figures. It is clearly shown that when the concrete compressive strength of the specimen increases,

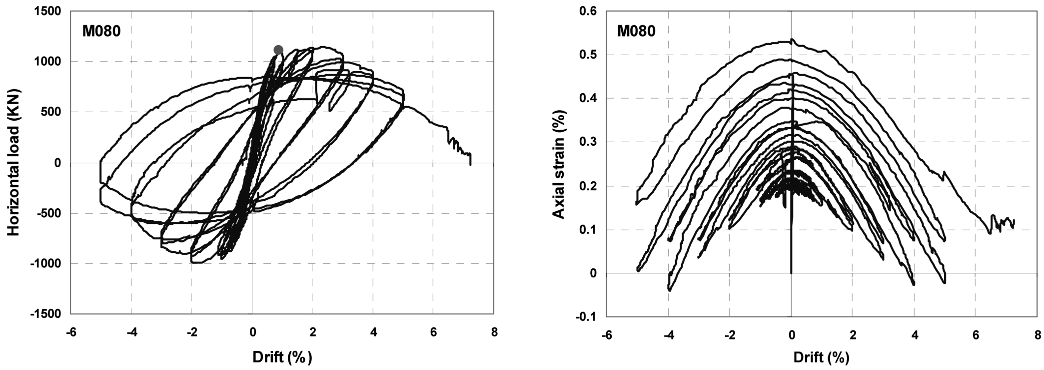

(a) 80MPa column

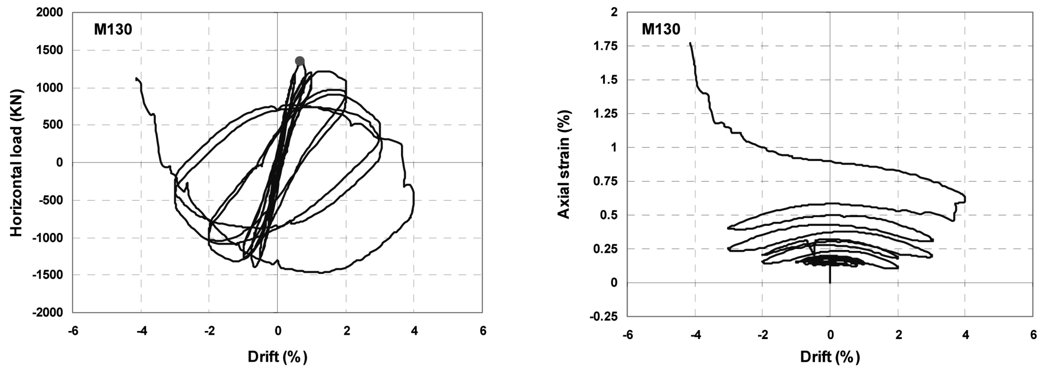

(b) 130MPa column

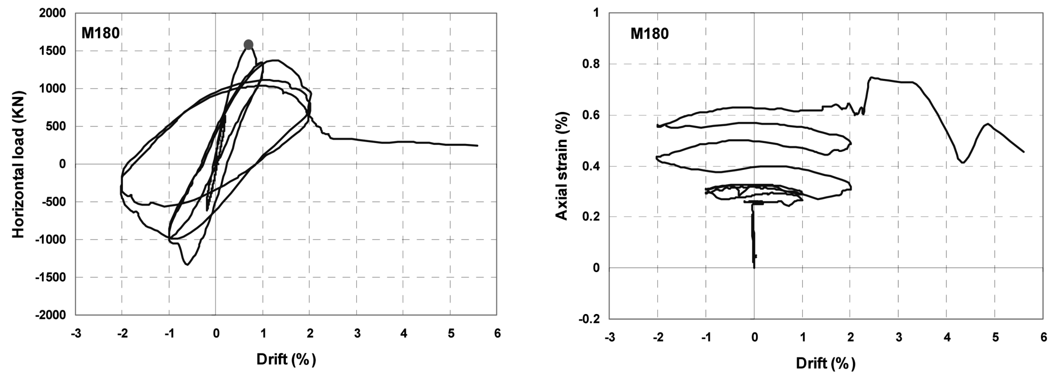

(c) 180MPa column

Fig. 7 Load-drift and axial strain-drift relationships for medium columns only shortening is observed as illustrated for specimen M130, M180, S130 and S180. In the same time it was observed that for a concrete compressive strength of 80 MPa, small size column S080 showed both shortening and elongation, where medium size column M080 showed nearly only shortening.

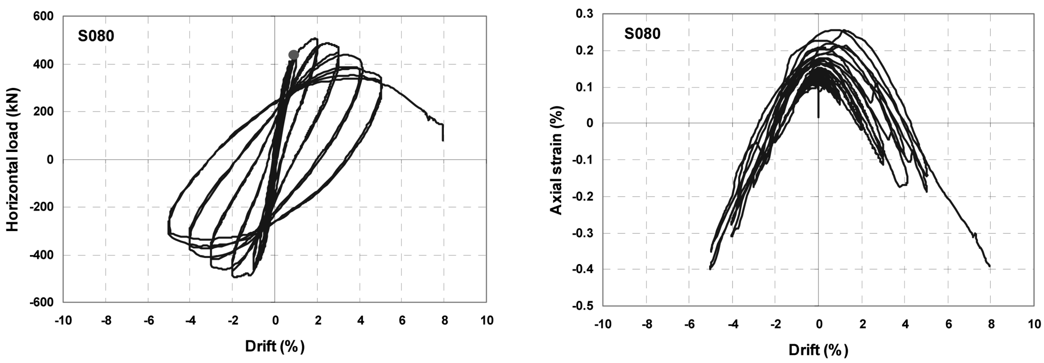

(a) 80MPa column

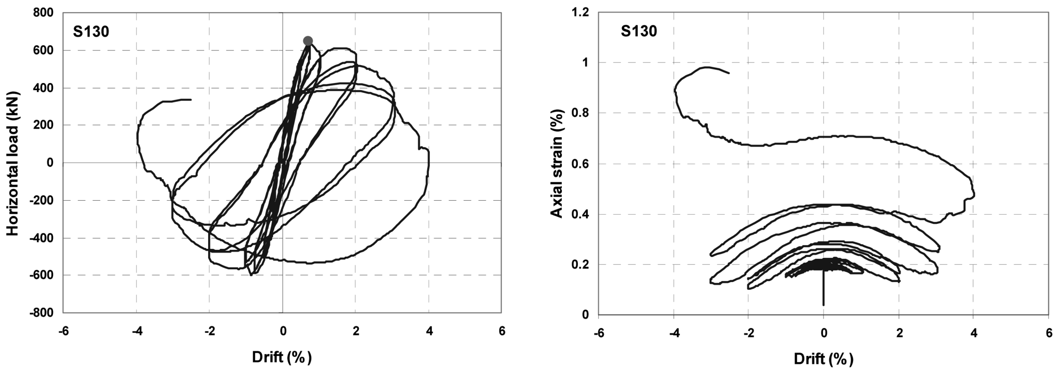

(b) 130MPa column

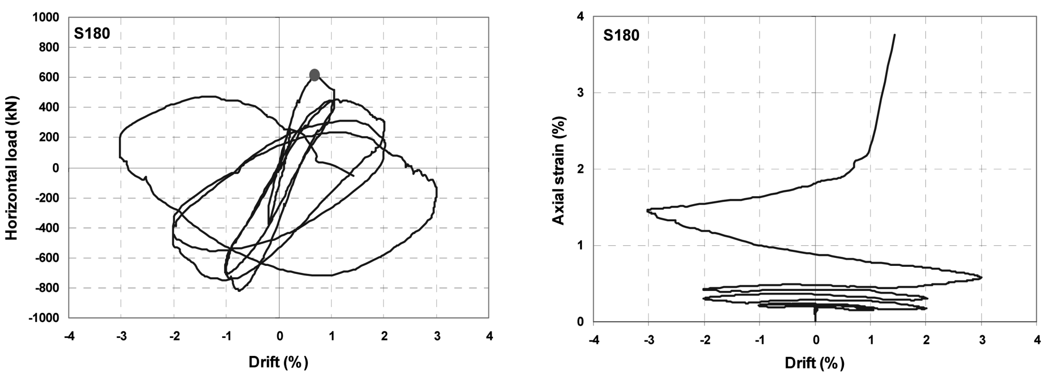

(c) 180MPa column

Fig. 8 Load-drift and axial strain-drift relationships for small columns

3.3 Size and concrete strength effects on the normalize moment-drift curves

Size effect on the moment-drift envelope curves was studied by comparing the normalized envelope curve of the medium size and the small size columns with the same concrete compressive strength. The normalization was done by dividing the original envelope curve by the maximum peak moment, M_{max}.

Fig. 9 shows a comparison between the medium and small size columns in term of the normalized moment-drift envelope curves. Only a slight difference was observes while comparing specimen with a concrete compressive strength of 180 MPa (M180 and S180) as shown in Fig. 9(c).

Effect of concrete compressive strength on the normalized moment-drift was clearly observed as illustrated in Figs. 10(a) and (b) for the small and medium size columns, respectively. The authors observed that the drift corresponding to the maximum moment decreased with an increase in the concrete compressive strength. Also, slope of the descending branch increased with an increase in the concrete compressive strength.

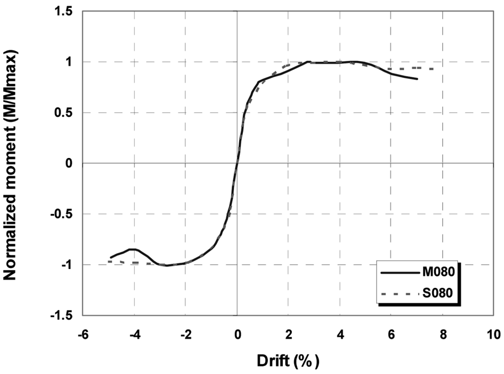

(a) 80MPa

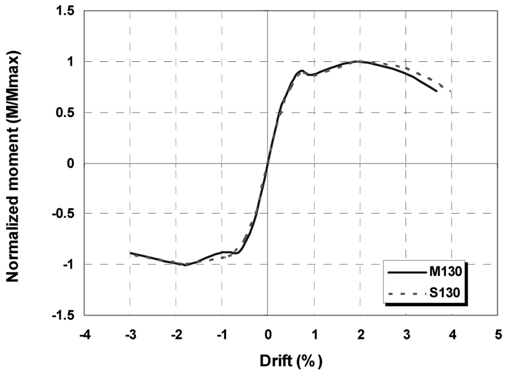

(b) 130MPa

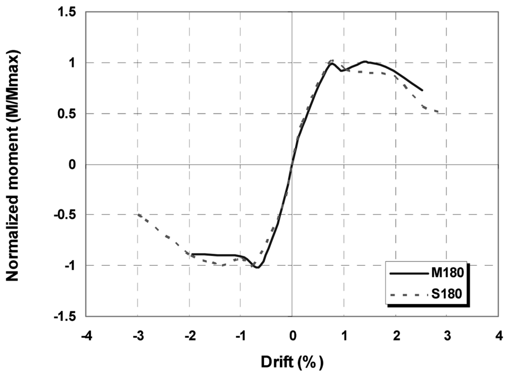

(c) 180 MPa

Fig. 9 Size effect on the moment-drift relationships

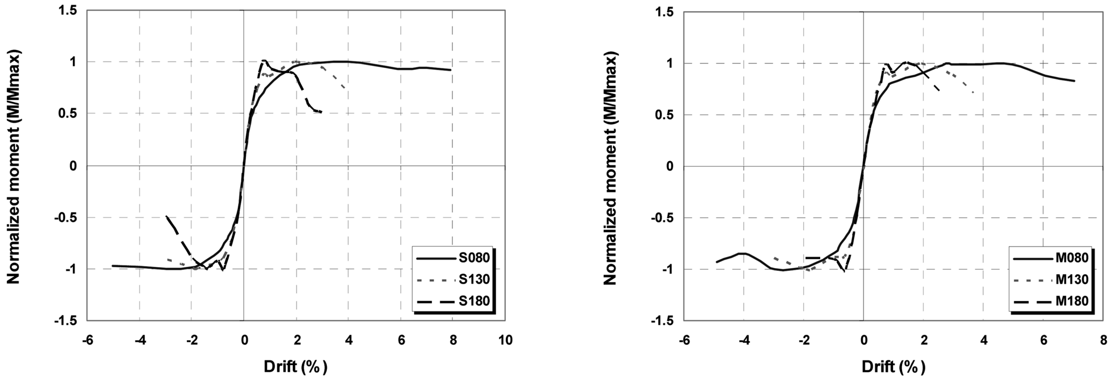

(a) Small size columns (b) Medium columns

Fig. 10 Concrete compressive strength effect on the moment-drift relationships

3.4 Curvature-drift variation

In total 15 displacement gauges were set at the lower part of the column to measure the imposed deformations as shown in Fig. 11. Curvature was computed for a height equal to the column depth, D, for all specimens. It was observed that the measured curvature for the small size columns was higher than that measured for the medium size columns which can be seen from Fig. 12. This statement can be illustrated as shown in Fig. 13.

However, and as it is shown in Fig. 14, for the same column's size and different concrete compressive strengths, no differences were observed in term of curvature for a drift varying between –2% and +2%.

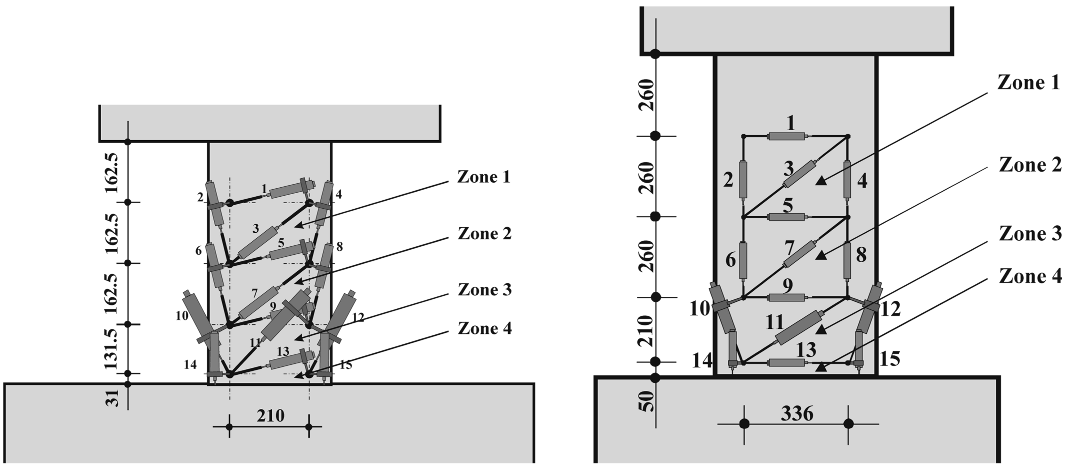

(a) Small columns (b) Medium columns

Fig. 11 Displacement gauges locations

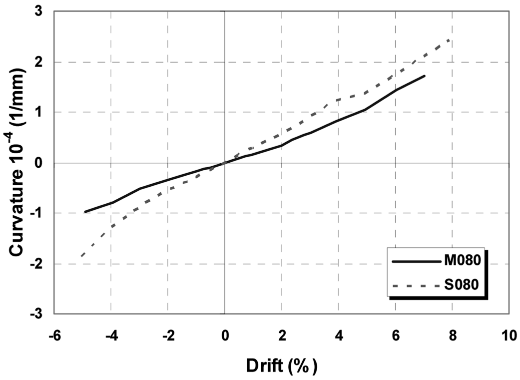

(a) 80MPa

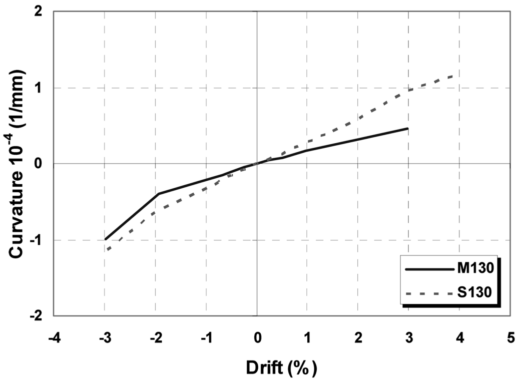

(b) 130MPa

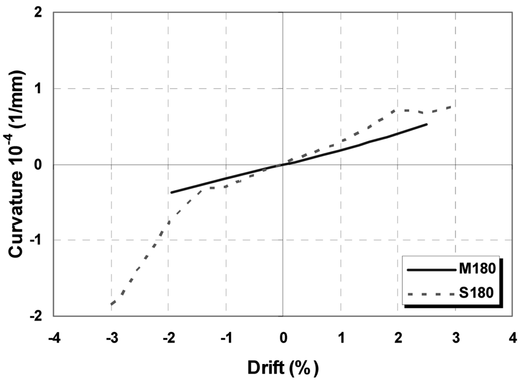

(c) 180MPa

Fig. 12 Curvature-drift variation

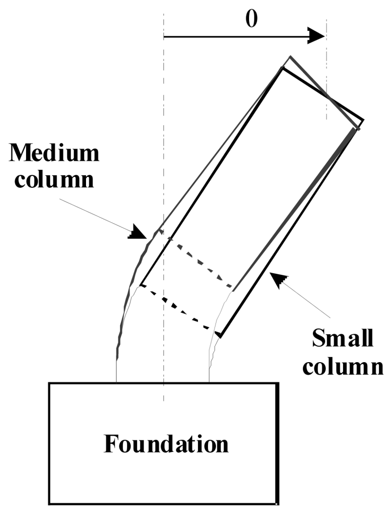

Fig. 13 Illustration of the observed deformation between the medium and small size columns

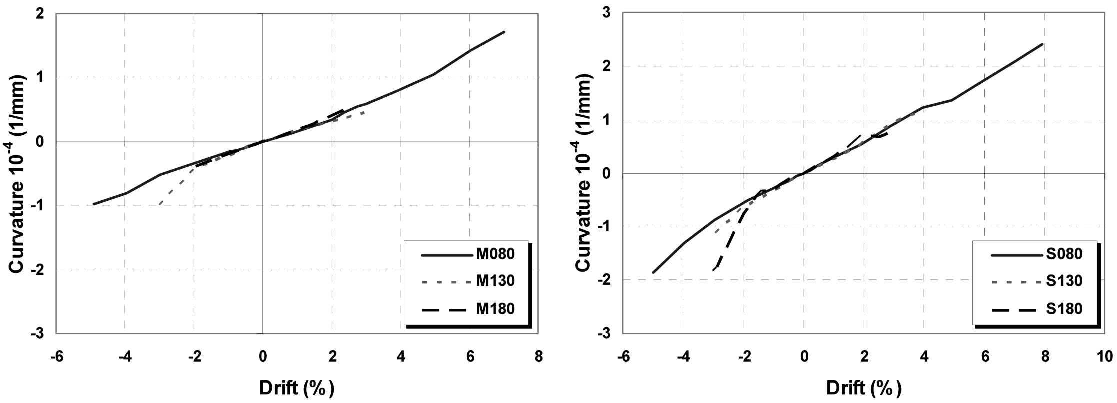

(a) Medium size (b) Small size

Fig. 14 Concrete compressive strength effect on curvature-drift variation

3.5 Damping factor variation

Variation of the equivalent viscous damping factor was computed using the first cycle loops to each of the imposed drift angle (Shibata 1976). The equivalent viscous damping, H_{eq}, was computed using the following expression

$$H_{eq} = \frac{1}{4\pi}\frac{\Delta W}{W_e} \tag{4}$$

where: ΔW is the area enclosed by one cycle of hysteresis loop and W_e is the equivalent potential energy.

Variation of the equivalent viscous damping is shown in Figs. 15 (a) and (b) for the small and the medium size column, respectively. From these two figures it can be drawn that the equivalent viscous damping increases with an increase in the concrete compressive strength. This increase can be attributed to the observed brittle failure of the reinforced concrete.

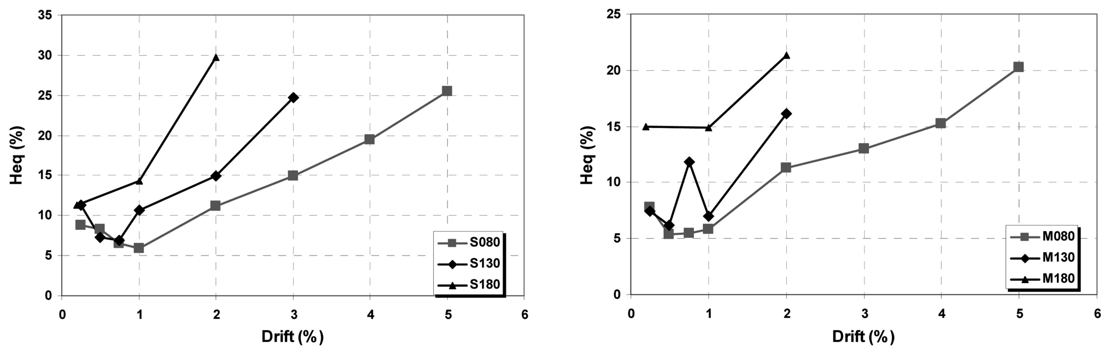

(a) Small size (b) Medium size

Fig. 15 Effect of concrete compressive strength on the damping factor variation

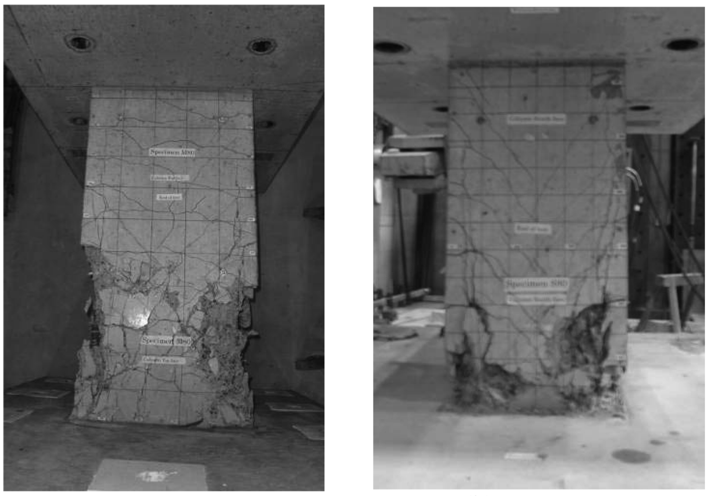

(a) M080 (b) S080

Fig. 16 Columns states at the end of the test

3.6 Observed damage

In general, the authors observed that the small size columns suffered less damage than the medium size columns as shown in Fig. 16. This statement was also observed in the past by the first author (Bechtoula 2005) while testing reinforced concrete columns with a concrete compressive strength varying between 30 and 40 MPa. Fig. 16 shows that for the small size columns, damage is concentrated at the lower part for a height less than the column depth, D. Whereas for the medium columns, the damage spreads for an average distance equal to 1.5D in height. This observation is in conformity with the illustration shown previously in Fig. 13.

3.7 Prediction of the moment-drift relationship

A relationship between the moment-drift envelope curve of the medium and the small size columns was established having the form of

$$M_M/M_S = (D_M/D_S)^{\beta} \tag{5}$$

where M_M, M_S, D_M and D_S are the moment and the column depth for the medium and small size columns, respectively.

β is a factor depending on the concrete compressive strength as shown in Fig. 17, f_c', and given by

$$\beta = 0.0035 f_c' + 3.13 (\text{in MPa}) \tag{6}$$

Eq. (6) was evaluated using the peak moments in Eq. (5) for the 3 types of reinforced concrete strengths.

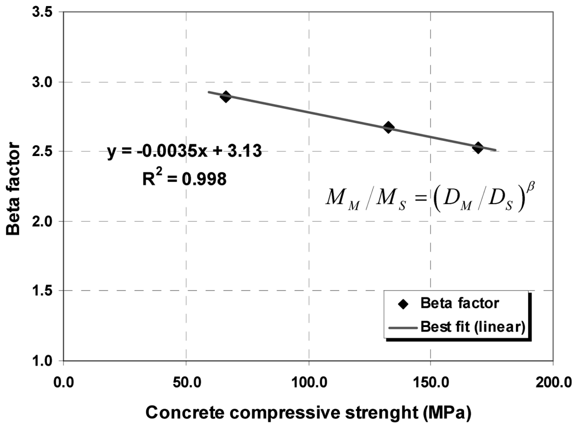

Fig. 17 Determination of the “Beta” factor using the peak moment

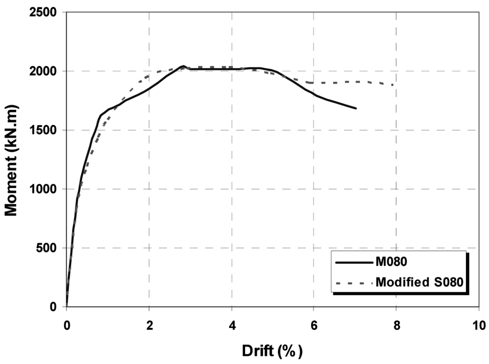

(a) 80MPa

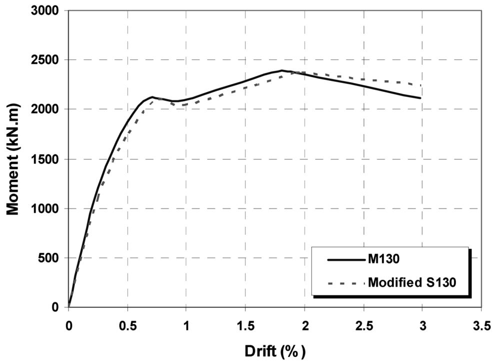

(b) 130MPa

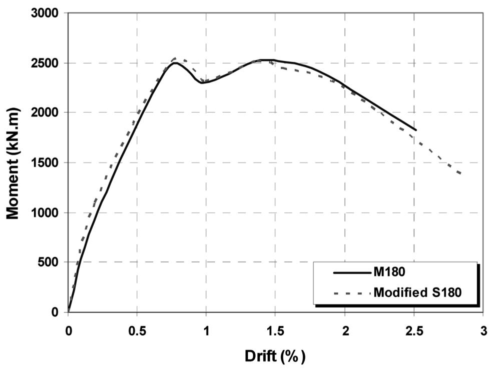

(c) 180MPa

Fig. 18 Prediction of the moment-drift envelope cure of the small size columns

Fig. 18 shows a comparison between the moment-drift envelope curves of the medium size columns and the modified moment-drift envelope curves of the small size columns using the proposed above equations, Eq. (5) and Eq. (6). As it can be observed, a good agreement is obtained along the full loading history.

4. Analytical results

4.1 ACI results

A comparison between the test results and the ACI results, in term of peak moment, is reported hereafter. The analytical results were evaluated using the ACI guidelines (ACI 2002) for 3 assumed concrete compressive strengths:

1. Theoretical values, which is based on the assumed design values.
2. Cylinder values that is based on the results of the cylinder tests.
3. Reduced values, which is based on the cylinder's results and taking into account the scale effect. This was done based on Kumagai *et al.* equation (Kumagai 2005).

Kumagai *et al.* suggested that the concrete compressive strength given by a cylinder test should be reduced in order to take into account the scale effect. The real concrete compressive strength that should be considered is given by

$$\sigma_c = k_d k_h \sigma_B \tag{7}$$

With

$$\begin{aligned} &(k_d = (d/100)^{\alpha}), \quad \text{and} \quad \alpha = -0.08 - \sigma_B/2000 \\ &k_h = 0.95 + 0.2(h/d_{\min})^{-2} \end{aligned} \tag{8}$$

where, σ_B is the cylinder concrete compressive strength with 100 mm diameter, σ_B is the reduced compressive strength. h is the clear height of the considered column, $d_{\min}$ is the minimum dimension of the column cross section and, d is the diameter of the equivalent circular section for the column.

Based on Eq. (7) and Eq. (8), the reduced concrete compressive strengths for the six columns were computed and summarized in Table 3.

Table 4 summarizes the experimental and the analytical peak moments for the six tested columns. The average peak moment ratio (Test/ACI) for the 6 specimens was 1.04, 1.10 and 1.27 using the 3 concrete compressive strengths, respectively. Kumagai *et al.* equation underestimated the test results by 27% while this value is only 10% using the cylinder test values. For illustration, Fig. 19 shows a comparison between the ACI results using the cylinder concrete compressive strengths and the test results.

Table 3 Reduced concrete compressive strength

Column	σ_B (MPa)	h (mm)	dmin (mm)	d (mm)	α	k_d	k_h	σ_c
M080	65.5	1040	520	586.76	-0.11	0.82	1.0	53.7
M130	130.4	1040	520	586.76	-0.15	0.77	1.0	100.9
M180	168.0	1040	520	586.76	-0.16	0.75	1.0	125.7
S080	67.5	650	325	366.72	-0.11	0.86	1.0	58.2
S130	134.9	650	325	366.72	-0.15	0.83	1.0	111.4
S180	170.4	650	325	366.72	-0.17	0.81	1.0	137.5

Table 4 Test and ACI peak moment results using the three assumed concrete strengths

			Bending moment (KN.m)					
			f'c: Theoretical		f'c: Cylinder		f'c: Reduced	
Column	Peak	Test	ACI	Test/ACI	ACI	Test/ACI	ACI	Test/ACI
M180	Positive	2514.2	3007.4	0.84	2833.0	0.89	2294.2	1.10
	Negative	-2056.2	-3007.4	0.68	-2833.0	0.73	-2294.2	0.90
M130	Positive	2271.4	2318.6	0.98	2323.9	0.98	1933.3	1.17
	Negative	-2373.7	-2318.6	1.02	-2323.9	1.02	-1933.3	1.23
M080	Positive	2034.0	1646.6	1.24	1452.8	1.40	1279.8	1.59
	Negative	-1729.3	-1646.6	1.05	-1452.8	1.19	-1279.8	1.35
S180	Positive	589.1	731.8	0.80	700.0	0.84	601.0	0.98
	Negative	-765.8	-731.8	1.05	-700.0	1.09	-601.0	1.27
S130	Positive	676.2	566.5	1.19	582.7	1.16	509.0	1.33
	Negative	-622.5	-566.5	1.10	-582.7	1.07	-509.0	1.22
S080	Positive	522.2	402.5	1.30	361.7	1.44	328.0	1.59
	Negative	-502.2	-402.5	1.25	-361.7	1.39	-328.0	1.53
			Average	1.04	Average	1.10	Average	1.27

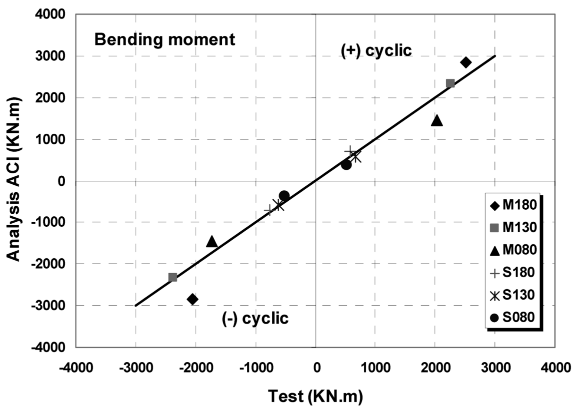

Fig. 19 Comparison between ACI and test results using cylinder results

4.2 Fiber model results

Behavior of a plastic hinge zone was predicted using a simple fiber model developed in our laboratory. Section analysis was carried out assuming Bernoulli's theory (plane sections remain plane) for concrete and longitudinal steel. The column cross section was subdivided into concrete fiber elements and reinforcing steel fiber elements. Section response was obtained by integrating all fiber element stresses and stiffness. Steel fiber elements followed Nakamura's stress-strain relation (Nakamura 1977), whereas concrete fiber elements followed Popovic's stress-strain relation (Popovics 1997). Concrete strength enhancement was taken into account using Sakino's *et al.* equation (Sakino 1994). More details about this fiber model can be found elsewhere (Bechtoula 2003).

Fig. 20 and Fig. 21 show a comparison between the test and the fiber model results in term of moment-drift and axial strain-drift relationships for the small and medium size columns, respectively.

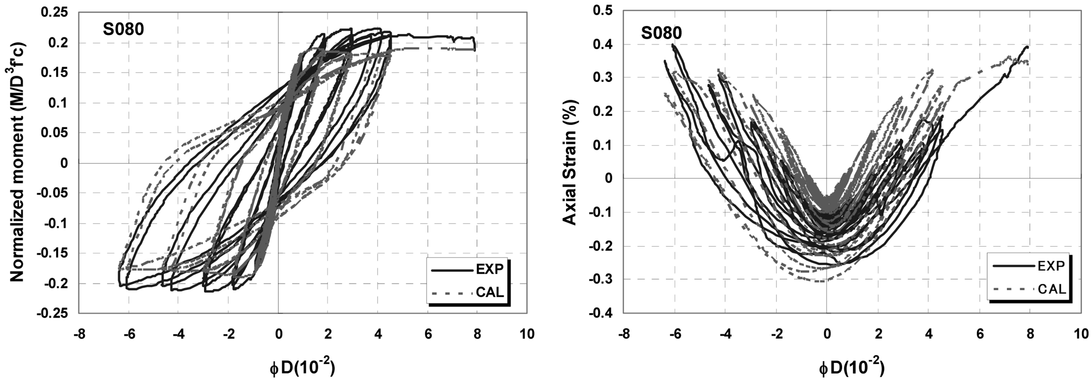

(a) 80MPa

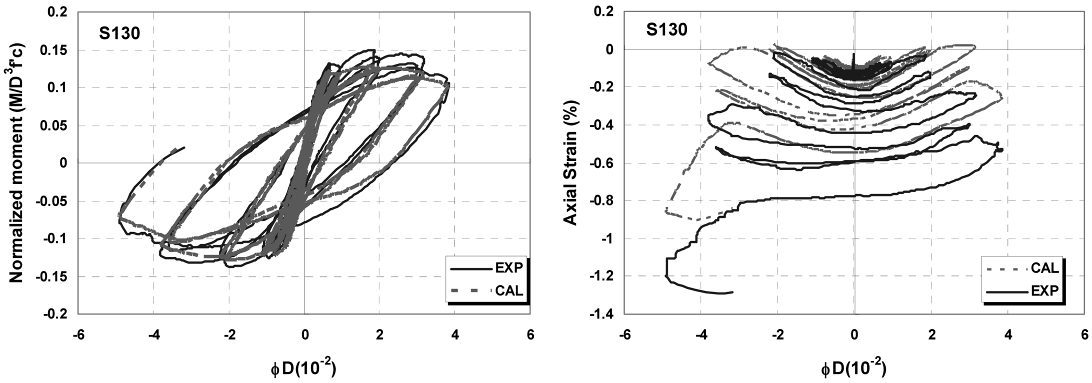

(b) 130MPa

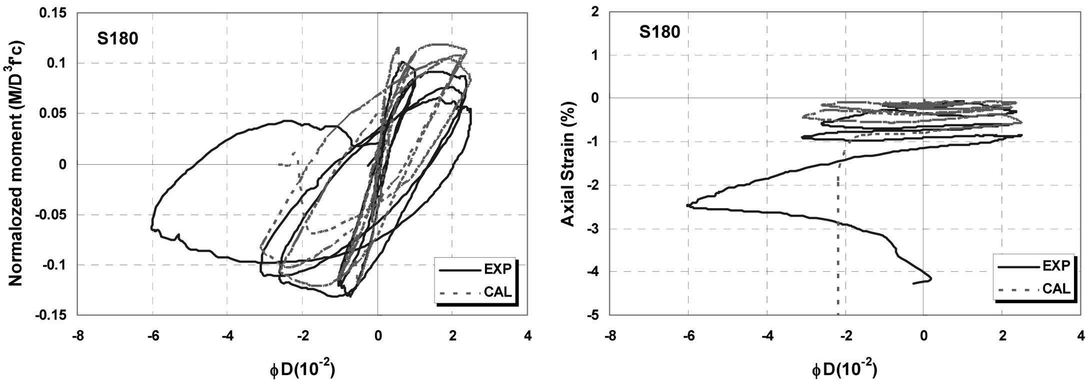

(c) 180MPa

Fig. 20 Fiber model and test results for the small size columns

As a general trend, a good estimation was obtained especially for the moment-drift relationships of the 6 specimens. However, analytical axial strain for the medium size columns (M080, M130 and M180) underestimated the experimental results as shown on the right side of Fig. 21.

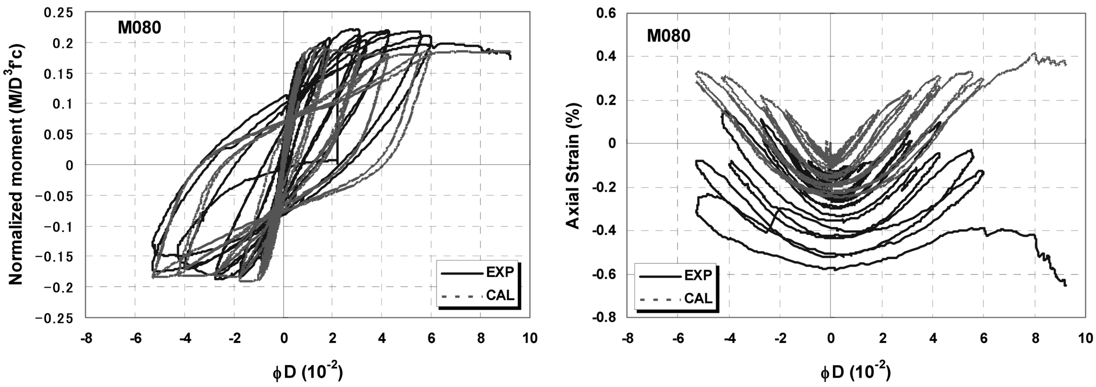

(a) 80MPa

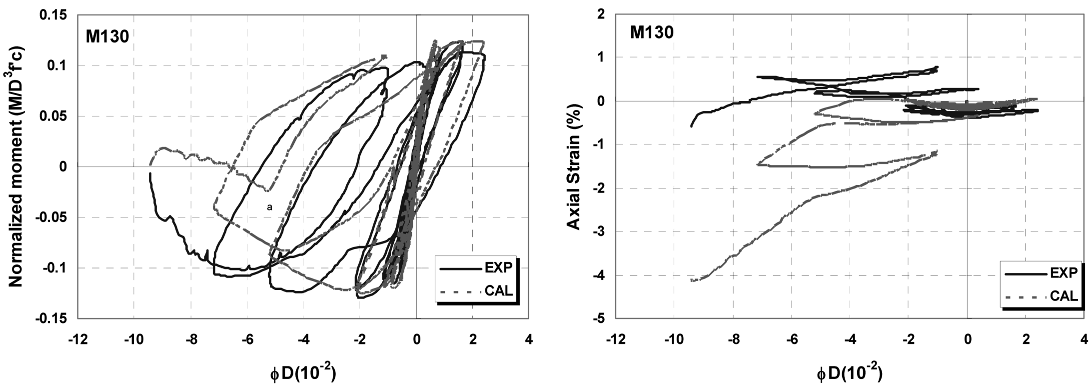

(b) 130MPa

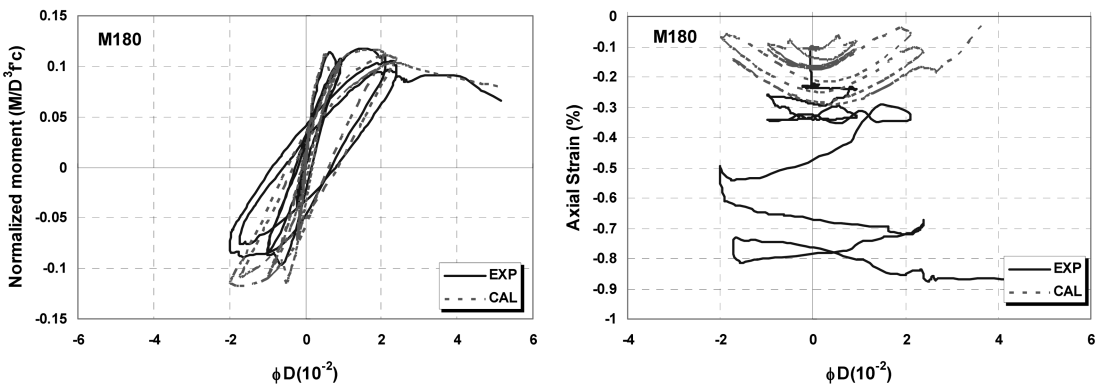

(c) 180MPa

Fig. 21 Fiber model and test results for the medium size columns

5. Conclusions

To investigate the seismic performance of high strength reinforced concrete columns under cyclic loadings, six specimens of which three had a cross section of 325 × 325 mm and the three other had a cross section of 520 × 520 mm were designed, constructed and tested at Kyoto University. Design concrete compressive strength was 80, 130 and 180 MPa. Shear span ratio and normalized axial load were identical for the six specimens. The experimental results showed that for specimens made of 180 MPa concrete compressive strength, spalling of cover concrete was very brittle followed by a significant decrease in strength. Curvature, evaluated at the base of the column for a height equal to the column depth, was much important for the small size columns than for the medium size columns. This difference in curvature distribution is attributed to the scale effect. Concrete compressive strength had no effect on the curvature distribution for a drift ratio varying between -2% and 2%, but it had an effect on the drift corresponding to the peak moments which decreased while the concrete compressive strengths increased. Also, an increase of the concrete compressive strength is followed by an increase of the equivalent viscous damping.

Based on the cylinder test results, an equation for evaluating the concrete Young's modulus was proposed. This equation agreed well with the formula proposed by Tomosawa *et al.* Also, a simple equation was suggested for evaluating the moment-drift envelope curves for medium size columns using those obtained from small size columns. This equation was used for the three columns with different concrete compressive strengths and gave very good results. The main feature of this equation is its simplicity in practice, since it is based only on the geometrical and material characteristics of the columns.

Analytical investigation was carried out using the ACI code and a fiber model developed by the authors. Using the ACI code with the concrete cylinder's compressive strength values, the peak moments ratios, Test/ACI, varied between 0.73 to 1.44 with an average of 1.10 for the six specimens. These values were, respectively, 0.90, 1.59 and 1.27 using the reduced concrete compressive strength as suggested by Kumagai *et al.*

Moment-drift and axial strain-drift hysteresis curves were predicted with a good accuracy using the fiber model. However, inaccurate analytical axial strain values were obtained for the medium size columns.

Acknowledgements

The authors are thankful to Mr. M. SAKASHITA, Mr. S. SHIBATA, Mr. T. MATSUDA, Mr. M. ODA and Mr. N. RYU former students at Kyoto University. The authors also acknowledge TAISEI and KAJIMA companies for their financial support. The first author is grateful to JSPS for their 2 years financial support as Post Doctor at Kyoto University.

References

ACI Committee 363 (2005), "High-strength concrete (ACI 363R)" by ACI Committee 363 – High-Strength Concrete, Seventh International Symposium on the Utilization of High-Strength/High-Performance Concrete, Special publication SP-228-5, Washington, D.C., USA.

ACI (2002), "American concrete institute building code requirements for structural concrete (ACI 318-02) and commentary (ACI 318R-02)", Reported by ACI Committee 318.

AIJ (1999), "Design guidelines for earthquake resistant reinforced concrete buildings based on inelastic concept", Architecture Institute of Japan.

Bechtoula, H. (2005), "Seismic performance of moderate or low rise reinforced concrete frame buildings", PhD thesis, Department of Architecture and Architectural Engineering, Kyoto University, Japan.

Bechtoula, H., Kono, S., Sakashita, M. and Watanabe, F. (2003), "Effect of number of cycles on damage progress for large scale columns under multiaxial loadings", *Proc. Japan Concrete Institute*, JCI, Kyoto, **25**(2), 355-360.

JICE (1988-1993), "New RC research development report (1988-1993)", Japan Institute of Construction Engineering.

Kumagai, H., Tozawa, M. and Kurose, Y. (2005), "Compression failure in reinforced concrete shear wall with ultra-high-strength materials", *Concrete Res. Technol., JCI*, **16**(3), 39.

Kuramoto, H., Kabeyasawa, T. and Shen, F.H. (1995), "Influence of axial deformation on ductility of high-strength reinforced concrete columns under varying triaxial forces", *ACI Struct. J.*, **92**(5), 610-618.

Martinez, S., Nilson, A.H. and Slate, F.O. (1982), "Spirally reinforced high strength concrete column", Research Report N°.82-10, Department of Structural Engineering, Cornell University, Ithaca, August.

Muguruma, H. and Watanabe, F. (1990), "Ductility improvement of high-strength concrete columns with lateral confinement", *Proceeding of the Second International Symposium on Utilization of High-Strength Concrete*, University of California, Berkeley, May 20-23.

Namiki, S., Sawai, N., Kuroha, K. and Hara, T. (1999), "Application of high-strength concrete with 1000 kgf/cm^2 to high-rise building", *Concrete Journal*, **37**(3), 35-38.

Nakamura, T. and Yokoo, Y. (1977), "Non-stationary hysteresis uniaxial stress-strain relations of wide flange steel: Part II-Empirical formulas", *Transaction of the Architectural Institute of Japan, AIJ*, **260**, 71-82.

Nishiyama, M. (1993), "Axial loading test on high strength concrete prisms confined by ordinary and high strength steel", Utilization of High Strength Concrete, Proceeding of High Strength Concrete Symposium, Norway, 322-329.

Popovics, S. (1997), "A numerical approach to the complete stress-strain curve of concrete", *Cement Concrete Res.*, **3**(5), 583-599.

Sakino, K. and Sun, Y. (1194), "Stress-strain curve of concrete confined by rectilinear hops", *J. Struct. Construct. Eng., AIJ*, **461**, 95-104.

Shibata, A. and Sozen, M.A. (1976), "Substitute-structure method for seismic design in R/C", *J. Struct. Div.*, ASCE, **102**(ST1), 1-18.

Tomosawa, F. and Noguchi, T. (1995), "Relationship between compressive strength and modulus of elasticity of high strength concrete", *J. Struct. Constr. Eng.*, *AIJ*, **474**, 1-10.